

STRUCTURAL STUDIES OF MATERIALS FOR HYDROGEN STORAGE

Final report - High Resolution SR-PXD: 01-01-805 Beamline BM01B

Initial comment

The Physics Department at Institute for Energy Technology has a strong activity on hydrogen storage materials, involving many national and international collaborators. The strong position of the group is to a high degree owing to the good access to neutrons for powder neutron diffraction (PND) using the diffractometer PUS at the Institute's research reactor JEEP II.

Synchrotron power X-ray diffraction (SR-PXD) is an invaluable supplement to PND due to the superior speed and resolution. The data acquisition times are typically 3 orders of magnitude shorter using the MAR345 image plate at BM01A compared to PUS at JEEP II. This allows in-situ investigations of chemical reactions that we cannot possibly follow with PND. The very high resolution offered at BM01B enables indexing and space group determination from complex structures where the problem with peak overlapping makes the task unmanageable with PND- or laboratory PXD data.

Thus, the predictable, long-term access to the beam lines at SNBL through the long-term projects 01-01-805 and 01-02-862, has been an invaluable supplement to our neutron diffraction facilities and the rest of our experimental activity.

This final report summarizes the obtained results for the long-term project 01-01-805.

Ca₃(BD₄)₃(BO₃) – a novel calcium borohydride borate

Ca(BH₄)₂ is considered an attractive hydrogen storage material due to its high gravimetric capacity and expected thermodynamic properties suitable for mobile hydrogen storage applications. The compound is expected to decompose to CaH₂ and CaB₆ accompanied by H₂ release. However, experimental work has shown a more complex pathway with formation of unknown intermediate products.

One such intermediate phase was first identified in the previous long-term project and preliminary suggested to be a new modification of Ca(BH₄)₂, tentatively named “ δ -Ca(BH₄)₂” (see final report for previous long-term project 01-02-772). A sample of this phase in almost pure form was produced in our home laboratory by using a procedure with repeated heating cycles. The sample was measured with the MAR345 image plate detector at BM01A and with HR-SR PXD at BM01B. The data could be indexed in an orthorhombic cell with unit cell parameters $a = 8.995 \text{ \AA}$, $b = 8.052 \text{ \AA}$ and $c = 11.767 \text{ \AA}$. The structure was solved in space group $Cmc2_1$ and identified as Ca₃(BD₄)₃(BO₃). The Rietveld refinement fit and reflection profiles are shown in Figure 1, and the structure is shown in Figure 2. The stability of the structure at ambient conditions is confirmed by DFT calculations, and the co-existence of BD₄ and BO₃ complexes are confirmed by IR spectroscopy.

Ca₃(BD₄)₃(BO₃) is the first example of a product from a borohydride oxidation containing both B-H and B-O bonds. It thus represents a novel category of compounds completely different from the hydroxoborate products that form upon borohydride

hydrolysis. The result represents an important contribution to fundamental boron chemistry and could provide insight to the reaction mechanisms encountered during borohydride oxidation.

The results have been published in Journal of Materials Chemistry [1].

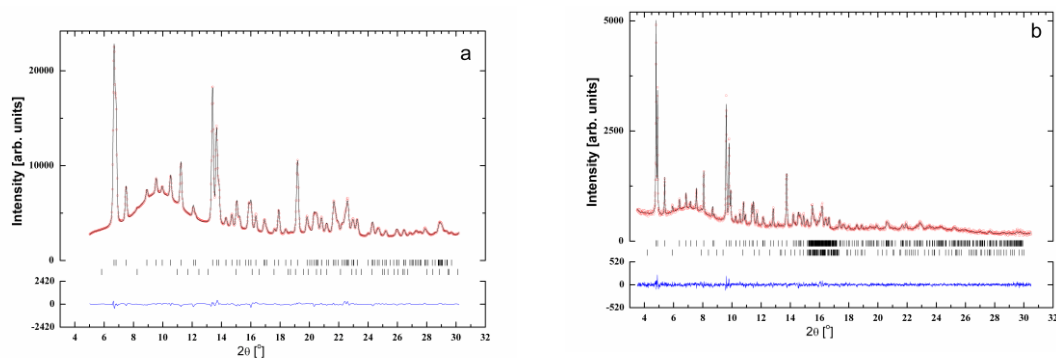


Figure 1: Rietveld refinement profiles for $\text{Ca}_3(^{11}\text{BD}_4)_3(^{11}\text{BO}_3)$ measured with (a) MAR345 image-plate set-up at BM01A and (b) high resolution diffractometer at BM01B. The figures show observed (circles), calculated (upper line) and difference (bottom line) profiles. Bars indicate the position of Bragg reflections for $\text{Ca}_3(^{11}\text{BD}_4)_3(^{11}\text{BO}_3)$ (upper) and $\beta\text{-Ca}(^{11}\text{BD}_4)_2$ (lower).

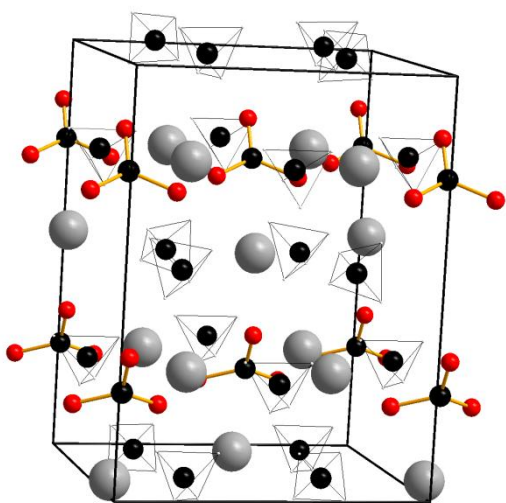


Figure 2: The crystal structure of $\text{Ca}_3(^{11}\text{BD}_4)_3(^{11}\text{BO}_3)$. Ca-atoms are shown as large spheres, oxygen as red spheres, and BD_4 anions as polyhedra.

The crystal structure of alpha- and beta-Y(BD₄)₃

The solvent adducts of rare-earth metal borohydrides have attracted considerable interest in recent years because of their highly selective catalytic activities towards certain organic reactions. Very little is known about the unsolvated rare-earth borohydrides, however, with respect to structure, catalytic activity and especially their potential use as solid state hydrogen storage materials.

The mechanochemical reaction between LiBD₄ and YCl₃ in ratios of 3:1 and 4:1 led to the formation of Y(BD₄)₃ in the form of several polymorphs. The structure of α -Y(BD₄)₃ was re-determined from doubly substituted (¹¹B, D) samples using PND data. Post annealing of the as-prepared material under deuterium resulted in a phase transformation at temperatures above 180 °C into β -Y(BD₄)₃. High-resolution SR-PXD data of a post-annealed sample were collected at BM01B and used for indexing and space group determination ($a=11.0086(1)$ Å; space group *Fm-3c*). The data were used in conjunction with PND data obtained from the PUS diffractometer at the JEEP II reactor (Kjeller, Norway) for ab-initio structure determination using the global optimization approach. The structure model was refinement according to the Rietveld method (Figure 3).

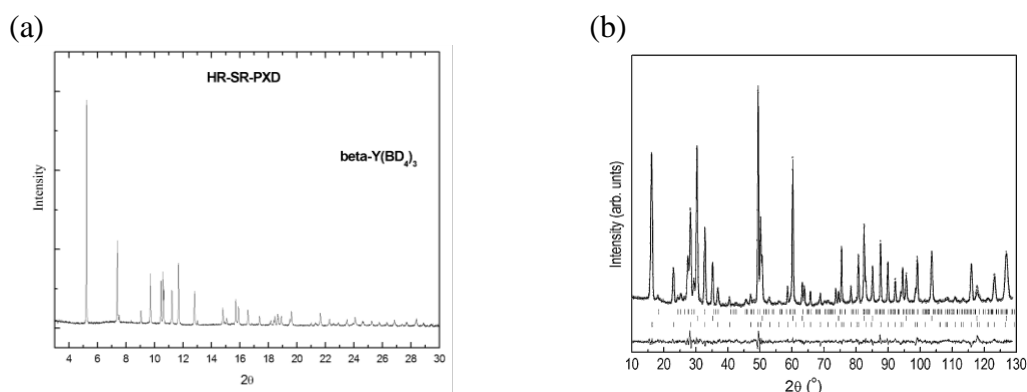


Figure 3: High-resolution SR-PXD data (a) and Rietveld fit of β -Y(BD₄)₃ for PND data (b). Upper, middle and lower tick marks show Bragg peaks from LiCl, LiBD₄ and β -Y(BD₄)₃, respectively.

The structure of β -Y(BD₄)₃ consists of Y³⁺ cations that are octahedrally surrounded by six [BD₄]⁻ anions. The local coordination scheme can be identified as [12D+6B]. It is obtained via twelve Y-D contacts through the edges of each BD₄ tetrahedron (Figure 4a) as well as six Y-B contacts in the form of an ideal and undistorted Y-B-octahedron (Figure 4b).

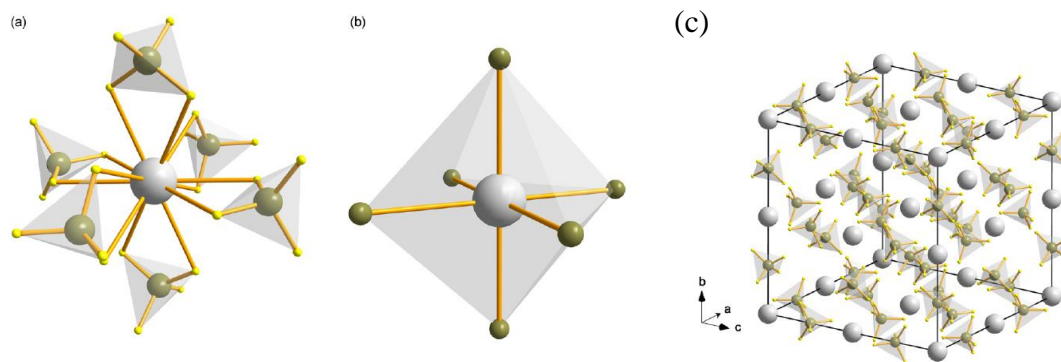


Figure 4 Local geometry around the central Y^{3+} cation in β - $Y(BD_4)_3$ emphasizing the [12D+6B] overall coordination (a and b). Unit cell content of β - $Y(BD_4)_3$ in space group $Fm-3c$ (c).

The results have been published in Journal of Alloys and Compounds [2].

The crystal structure of $LiCe(BD_4)_3Cl$

The mechanochemical reaction between $LiBH_4$ and $CeCl_3$ in a molar ratio of (3:1) has been reported to lead to the formation of the lanthanide borohydride $Ce(BH_4)_3$. Our results obtained under identical experimental conditions indicate the formation of the first mixed-metal, mixed-anion lanthanide borohydride, $LiCe(BH_4)_3Cl$, instead.

The doubly-substituted (^{11}B , D) material was measured by high-resolution SR-PXD (BM01B) and PND (PUS, JEEP II). A structure model in the cubic space group $I-43m$ ($a = 11.59159(16)$ Å) was later used for a combined Rietveld refinement (Figure 5).

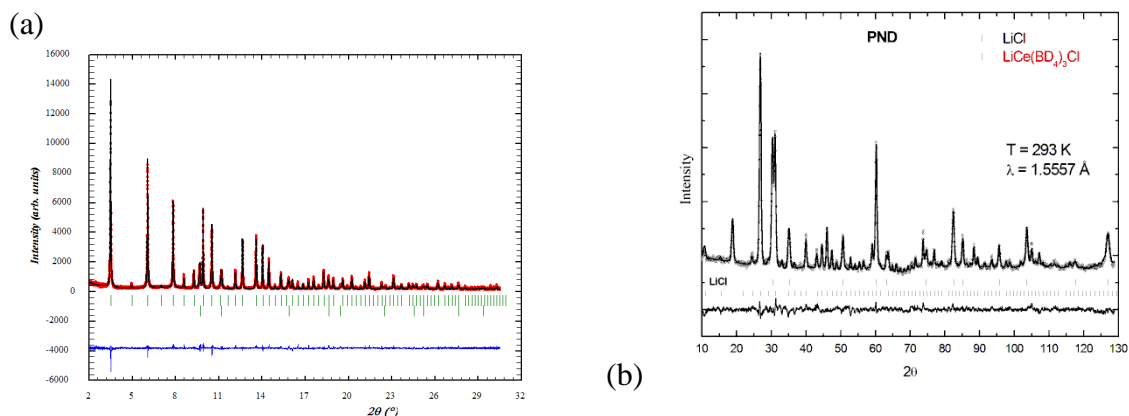


Figure 5: Rietveld fits of $LiCe(BD_4)_3Cl$ to high-resolution SR-PXD data (a) and PND data (b). Tick marks represent Bragg peaks from $LiCe(BD_4)_3Cl$ and $LiCl$ respectively.

The crystal structure and unit cell contents for $LiCe(BD_4)_3Cl$ are presented in Figure 6.

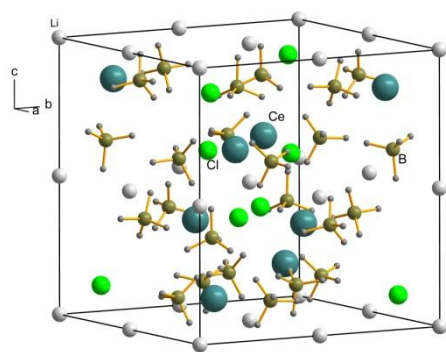
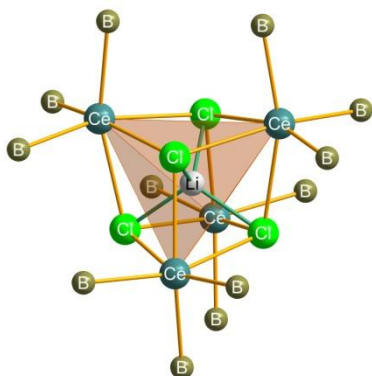


Figure 6: Unit cell content of $\text{LiCe}(\text{BD}_4)_3\text{Cl}$ in space group $I-43m$.

The structure can be envisioned as being composed of $\text{Ce}_4\text{-Cl}_4$ subunits forming a distorted hetero-cube. Each cerium atom is furthermore coordinated to 3 $[\text{BD}_4]$ groups resulting in an octahedral environment (Figure 7).

(a)



(b)

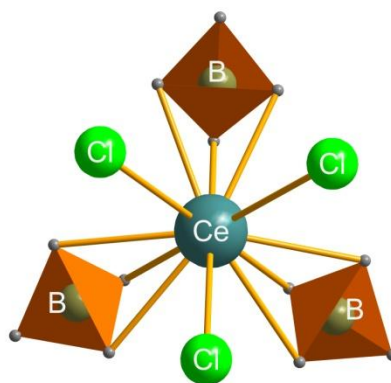


Figure 7: Local coordination scheme around the central Ce^{3+} cation in the structure of $\text{LiCe}(\text{BD}_4)_3\text{Cl}$ (a) with emphasis on Ce-D contacts (b).

The overall coordination scheme around the central cerium cation can be described as $[\text{9D}+3\text{Cl}]$ with Ce-D contacts being realized through tetrahedral faces of each $[\text{BD}_4]^-$ anion (Figure 8).

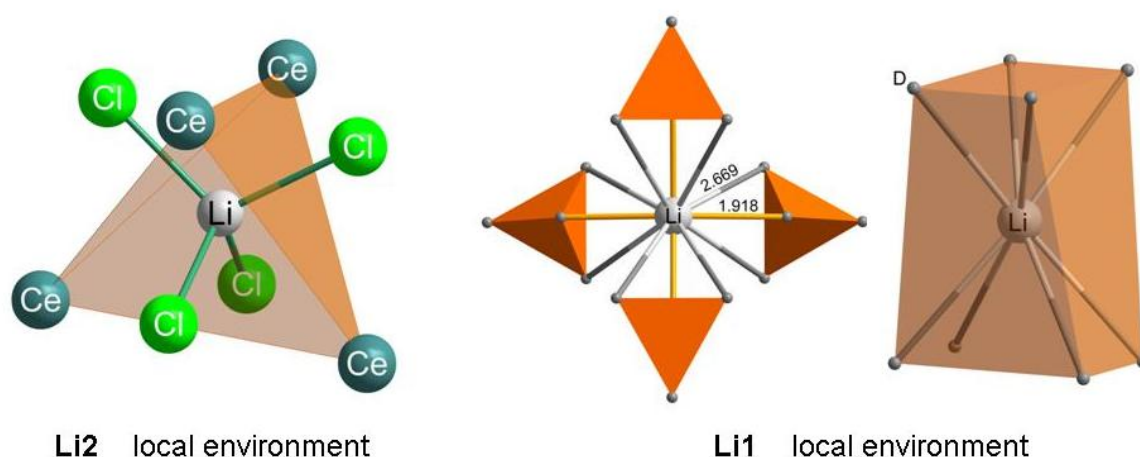


Figure 8: The local environment of the two independent Lithium ions in the structure of $\text{LiCe}(\text{BD}_4)_3\text{Cl}$. The Li1 position exhibits different Li-D contacts: 4 short distances of 1.918 Å (single-color) and 8 long distances of 2.669 Å (double-color).

The two crystallographically independent Li ions possess completely different coordination schemes: Li1 has a similar environment to that found in the orthorhombic phase of LiBH_4 and is tetrahedrally surrounded by 4 $[\text{BD}_4]$ groups. There exist 12 Li-D contacts that are realized through coordination of tetrahedral faces of each $[\text{BD}_4]$ tetrahedron to the Lithium cation. 4 of these Li-D contacts are short and around 1.91 Å in length, whereas the remaining 8 contacts are much longer and about 2.67 Å (Figure 6).

The second Lithium atom, Li2, occupies the central position inside the Ce-Cl hetero-cube subunit and is tetrahedrally surrounded by four Ce atoms and 4 Cl atoms with short Li-Cl bond distances of 2.193(5) Å and Ce-Cl bond distance of about 2.964(3) Å (Figures 6 and 8).

The results have been published in J. Phys. Chem C [3].

The mechano-chemical reaction between LiBH_4 and YbCl_3

Ball-milling is a feasible alternative to wet-chemical methods in order to synthesize borohydrides, since it allows preparation of these materials without the need for additional solvents. This eliminates the existence of intermediate solvent-adducts that have to undergo heat-treatment in order to obtain the solvent-free materials.

The mechano-chemical reaction between LiBH_4 and YbCl_3 in a molar ratio of (3:1) was found to proceed without gas evolution, which indicated that ytterbium was kept in its original trivalent state, and that the reaction was conducted without decomposition of the starting materials.

HR-SR-PXD (BM01B) and PND (PUS; JEEP II) data were collected on hydride and deuteride samples. The as-milled material possessed very broad peaks and could be indexed in a cubic unit cell with $a = 6.2008(8)$ Å in space group $P23$. Post-annealing under hydrogen/deuterium led to new materials/phases for temperatures above 100 °C. Figure 9 shows the SR-PXD and PND patterns for a sample annealed at 160 °C / 30 bar deuterium:

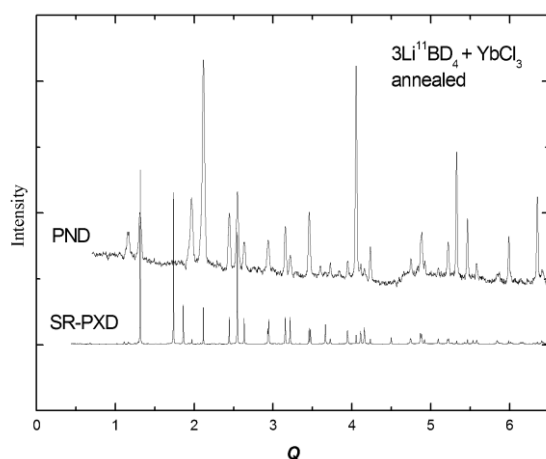


Figure 9: Intensity as a function of Q for a post-annealed mixture of $3\text{LiBD}_4\text{-YbCl}_3$ obtained by HR-SR-PXD (bottom) and PND (top).

The HR-SR-PXD data was used for indexing and space group assignment. Based on 19 reflections in the Q -range 1.25 – 6, a tetragonal unit cell with lattice parameters $a = 6.74552(12) \text{ \AA}$ and $c = 4.28216(8) \text{ \AA}$ was identified as a possible solution. Based on reflection conditions, $P4_2/nnm$ was then selected as the most probable space group. Interestingly, a LeBail intensity extraction performed on the PND data in this space group setting (and possible subgroups) showed the existence of several peaks that were not allowed, most prominently the first intensive peak in the PND data. This would indicate that either a) the unit cell is larger than seen by PXD, e.g. a lattice constant needs to be doubled, or b) the crystal symmetry is only pseudo-tetragonal and that in fact the system needs to be described in an orthorhombic or even lower symmetry due to different sublattice ordering of the weakly contributing BD_4 scatterers compared to the heavy atom ytterbium. Since the appearance of the PXD data is dominated by ytterbium, it appears that the true symmetry can only be obtained from a combination of SR-PXD - PND data sets.

This system is currently under investigation.

The mechano-chemical reaction between NaBH_4 and YCl_3

Ball-milling and cryo-milling experiments with mixtures of $\text{LiBH}_4 / \text{NaBH}_4$ and YCl_3 (4:1) were performed aiming at the synthesis of the mixed-metal borohydride $\text{Li/NaY}(\text{BH}_4)_4$. In the case of LiBH_4 as a borohydride source, the formation of $\text{Y}(\text{BH}_4)_3$ was observed instead. The use of NaBH_4 , however, led neither to the formation of $\text{Y}(\text{BH}_4)_3$ nor to $\text{NaY}(\text{BH}_4)_4$ as a final product. In-situ SR-PXD experiments performed at BM01A (see report for long-term project 01-02-862) on as-milled materials indicated the formation of several crystalline phases during heat treatment in the solid state, followed by thermal decomposition at temperatures above $350 \text{ }^\circ\text{C}$. Several attempts were undertaken to generate these crystalline phases ex-situ and to characterize them by powder diffraction. Figure 10 shows the HR-SR-PXD pattern of a post-annealed sample that was obtained by heating the as-milled material at a temperature of 225°C under 30 bar of hydrogen for 24 hours.

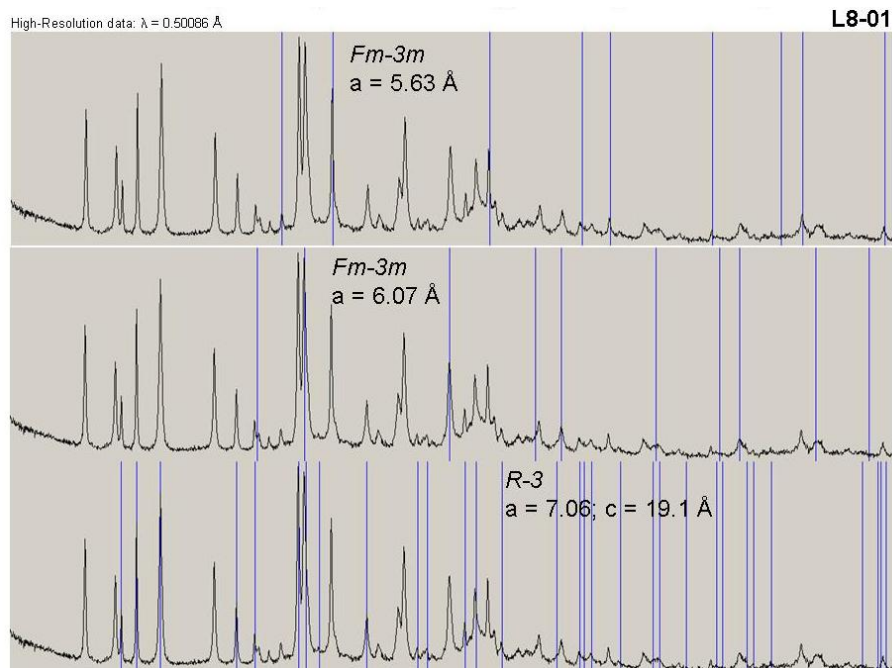


Figure 10: HR-SR-PXD pattern of a $4\text{NaBH}_4\text{-YCl}_3$ mixture annealed at $225 \text{ }^\circ\text{C}$ under 30 bar of hydrogen with indicated peak positions for NaCl (top), NaBH₄ (middle) and Na₃YCl₆ (bottom). The remaining peaks belong to a hitherto unknown phase.

Three phases could be identified from the HR-SR-PXD data: NaCl ($a=5.63 \text{ \AA}$, space group $Fm-3m$), NaBH₄ ($a = 6.07 \text{ \AA}$, space group $Fm-3m$), and a Na₃YCl₆-type phase ($a = 7.06 \text{ \AA}$, $c= 19.1 \text{ \AA}$, space group $R-3$), albeit with enlarged lattice constants compared to the published structure in the ICSD database (database-entry 300258: $a= 6.973(1) \text{ \AA}$, $c = 18.684(1) \text{ \AA}$). This could indicate that Cl-BH₄ anion substitution has occurred in the sample.

Assuming that the remaining peaks belonged to a single phase, they were indexed on basis of an orthorhombic unit cell ($a = 8.1218(2) \text{ \AA}$, $b = 6.5964(2) \text{ \AA}$, $c = 6.7565(2) \text{ \AA}$). Reflection conditions were found to be in agreement with space groups $Pmm2/Pmmm$.

Ravnsbæk et al. have recently demonstrated in an independent study that this phase is in fact a rare example of a mixed-metal, mixed-anion borohydride, namely NaY(BH₄)₂Cl₂.

The results will be included in a planned publication on transition metal- and rare earth-borohydrides.

Substitution of hydrogen by fluoride in AlD_3

AlD_3 , alane, is regarded as an interesting material for hydrogen storage due to its high gravimetric hydrogen content (10.8 wt%). In this study, fluorides were added to the synthesis of alane to investigate a possible substitution by the formation of a mixed solid solution phase like $\text{AlD}_{(3-x)}\text{F}_x$. Such anion substitution could change the stability and thermodynamics of alane.

Alane was made by cryomilling a mixture of $3\text{LiAlD}_4 + \text{AlCl}_3 \rightarrow 4\text{AlD}_3 + 3\text{LiCl}$. In two samples, either AlF_3 or NaF were added to the starting materials in a molar ratio 1:1 of D and F in the sample. In a third sample (sample 3) AlD_3 was premade by the above mentioned reaction and AlF_3 was added after the synthesis to see possible changes from the sample preparation conditions. The samples were cryomilled for 1 h in a Spex Freezer mill. High resolution PXD data was collected at SNBL station B. The samples were measured after 4 months of storage.

Sample 1: $3\text{LiAlD}_4 + \text{AlCl}_3 + 4\text{AlF}_3$

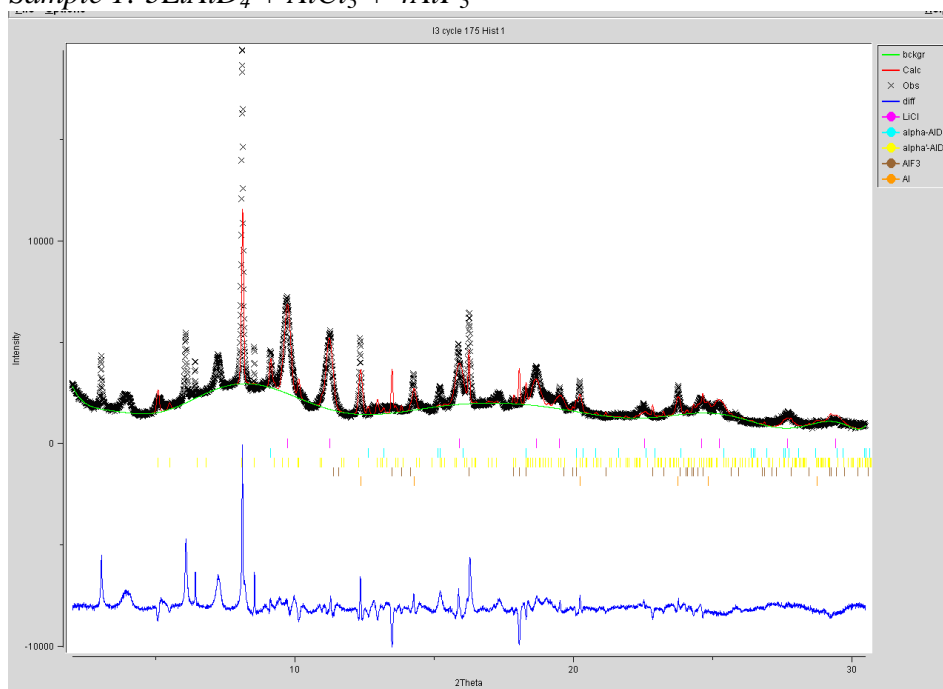


Figure 11: PXD of a mixture of $3\text{LiAlD}_4 + \text{AlCl}_3 + 4\text{AlF}_3$ after cryomilling and 4 months of storage.

The data show an increased content of Al compared to data from previously measured fresh samples. This indicates a decomposition of the AlD_3 during storage. The measured diffraction from the starting material AlF_3 did not correspond well to literature data, probably because of impurities or multiple phase composition (Figure 11). This made the data analysis difficult. But there are no clear changes in the cell parameters of AlD_3 to indicate possible F-substitution.

Sample 2: $3\text{LiAlD}_4 + \text{AlCl}_3 + 12\text{NaF}$

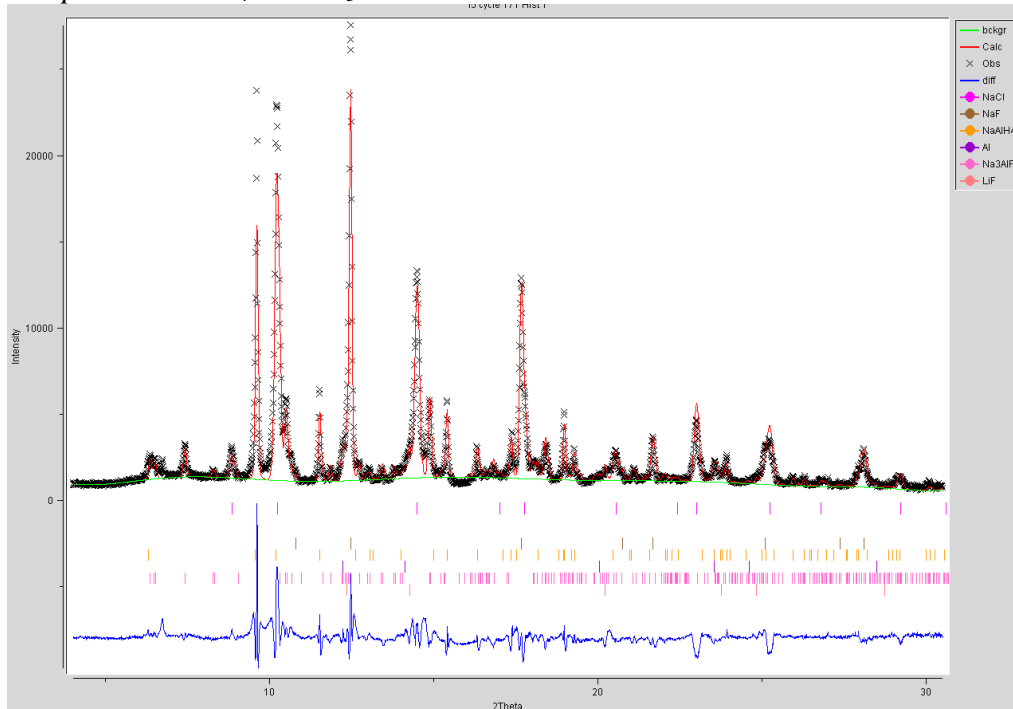


Figure 12: PXD of a mixture of $3\text{LiAlD}_4 + \text{AlCl}_3 + 12\text{NaF}$ after cryomilling and 4 months of storage.

The sample shows no content of AlD_3 . The addition of NaF favours formation of NaAlD_4 instead of AlD_3 (Figure 12). A fraction of Na_3AlF_6 is also found, in addition to NaCl , Al , NaF and possible reflections from LiF .

Sample 3: $\text{AlD}_3 + \text{AlF}_3$

In this sample AlF_3 was added after synthesis of AlD_3 and mixed by cryomilling. The sample contains more Al than sample 1 and a smaller fraction of AlD_3 , showing an increased decomposition of AlD_3 . The same problem of refining the diffraction from AlF_3 also holds for this sample and made the analysis difficult. No sign of anion substitution is seen.

The results have been published in Journal of Alloys and Compounds [4]

Investigation of possible anion substitution in $\text{Mg}(\text{BH}_4)_2$

Mixtures of $\text{Mg}(\text{BH}_4)_2 + \text{MgX}_2$ ($X = \text{Cl}, \text{Br}$) were ball-milled for 12h (280 rpm) and then annealed at 200 °C for 10 h under 10 bar H_2 . High resolution SR-PXD data were collected at BM01B at room temperature. SR-PXD data (Figure 13) shows that the peak positions from $\beta\text{-Mg}(\text{BH}_4)_2$ in the mixtures are shifted to higher angles by about 0.05 ° compared to pure $\beta\text{-Mg}(\text{BH}_4)_2$. The unit cell dimensions for $\beta\text{-Mg}(\text{BH}_4)_2$ were refined by the Rietveld method. The pure $\beta\text{-Mg}(\text{BH}_4)_2$ phase in sample (a) shows the following lattice constants: $a = 37.103 \text{ \AA}$, $b = 18.6328 \text{ \AA}$, $c = 10.9048 \text{ \AA}$, and these values are in agreement with those reported in the ICSD database. The unit cell parameters of $\beta\text{-Mg}(\text{BH}_4)_2$ in the mixtures are: $a = 36.878 \text{ \AA}$, $b = 18.5185 \text{ \AA}$, $c = 10.8145 \text{ \AA}$ for sample (b) and $a = 36.891 \text{ \AA}$, $b = 18.5100 \text{ \AA}$, $c = 10.8028 \text{ \AA}$ for sample (c), respectively. These smaller unit cell dimensions could be due to a substitution of BH_4^- (ionic radius $r = 2.05 \text{ \AA}$) by Cl^- ($r = 1.81 \text{ \AA}$) or Br^- ($r = 1.96 \text{ \AA}$).

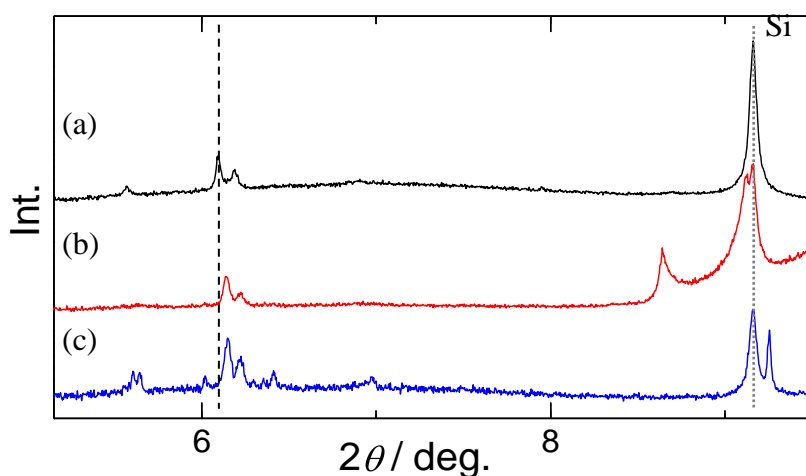


Figure 13: SR-PXD data ($\lambda = 0.50123 \text{ \AA}$) for (a) $\text{Mg}(\text{BH}_4)_2$ heated up to 300 °C under 10 bar H_2 atmosphere, (b) $\text{Mg}(\text{BH}_4)_2 + \text{MgBr}_2$ and (c) $\text{Mg}(\text{BH}_4)_2 + \text{MgCl}_2$ milled for 12h at 280 rpm and annealed at 200 °C for 10 h under 10 bar H_2 atmosphere. The samples contained Si powder as an internal standard from preliminary lab-PXD measurements.

$\text{Mg}(\text{BH}_4)_2$ was ball milled with MgI_2 in a 1:1 molar ratio to possibly partly substitute the BH_4^- unit of $\text{Mg}(\text{BH}_4)_2$ by I^- and make a mixed phase $\text{Mg}(\text{BH}_4)_{2-x}\text{I}_x$. The mixture was hand-ground for 10 min or ball milled for 30 min, 1h, 2h and 12h at 280 or 500 rpm to see possible substitution. High resolution SR-PXD data of the samples was collected at beamline BM01B, and the data currently awaits analysis..

The work is still in progress..

Phase transformations in chlorine-substituted NaBH_4

Samples of $\text{Na}(\text{BH}_4)_{1-x}\text{Cl}_x$ with any value of x can be prepared by ball milling of NaBH_4 and NaCl in the proper ratio. Pure NaBH_4 is reported to have a phase transition at 190 K. Simultaneous SR-PXD and Raman measurements of NaBH_4 were performed at BM01B at ambient temperature and 110 K. Both data methods confirm that a phase transformation has taken place (Figure 14).

Similar measurements were performed on $\text{Na}(\text{BH}_4)_{1-x}\text{Cl}_x$ with $x = 0.25$ and 0.75 . Neither diffraction nor Raman spectroscopy indicate symmetry lowering at 110 K, thus demonstrating that the chloride substitution has a pronounced influence on the phase transition temperature.

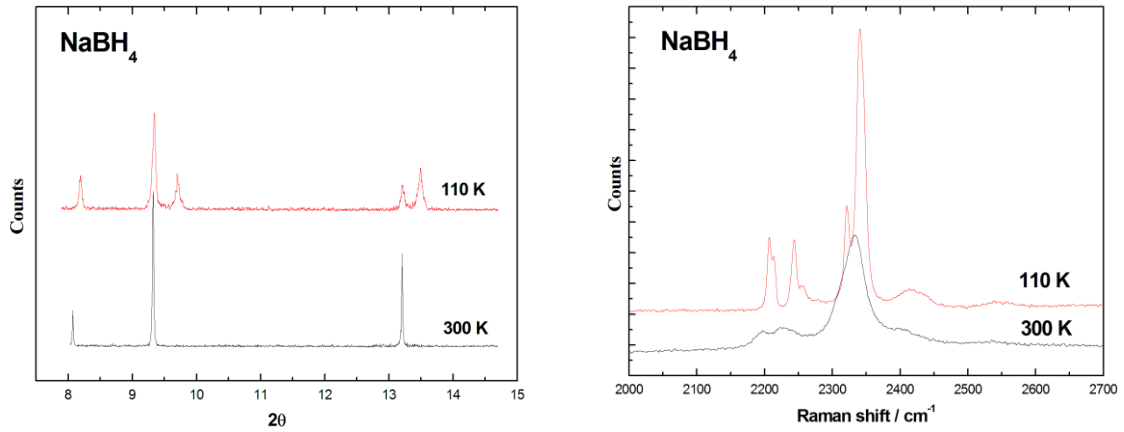


Figure 14: SR-PXD (left) and Raman spectroscopy (right) of NaBH_4 at 300 K and 110 K.

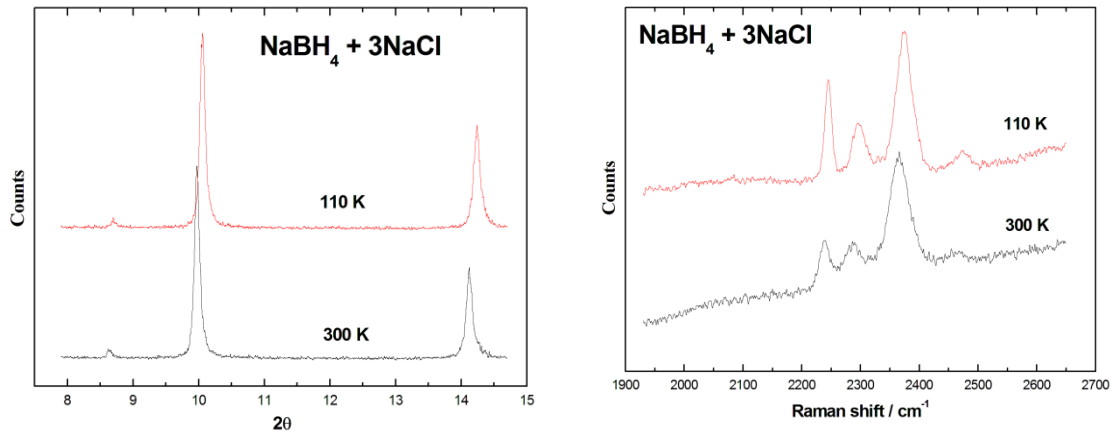


Figure 15: SR-PXD (left) and Raman spectroscopy (right) of $\text{Na}(\text{BH}_4)_{1-x}\text{Cl}_x$ at 300 K and 110 K.

The structure and phase transition will be further investigated by powder neutron diffraction at IFE, where temperatures down to 9 K can be reached, and the results will be published later in 2012.

The crystal structure of $\text{Ca}(\text{AlD}_4)_2$

Solvent-free $\text{Ca}(\text{AlD}_4)_2$ was synthesized by ball milling of CaD_2 and AlD_3 in a molar ratio of 1:2. The crystal structure of $\text{Ca}(\text{AlD}_4)_2$ had been predicted by computational methods to take the orthorhombic $\text{Ca}(\text{BF}_4)_2$ -type structure. However, this had not been experimentally verified.

SR-PXD data collected at BM01B and PND data collected at the PUS instrument at IFE (Kjeller, Norway) were used in a simultaneous Rietveld refinement of the crystal structure (Figure 16). The refinements confirm the predicted structure.

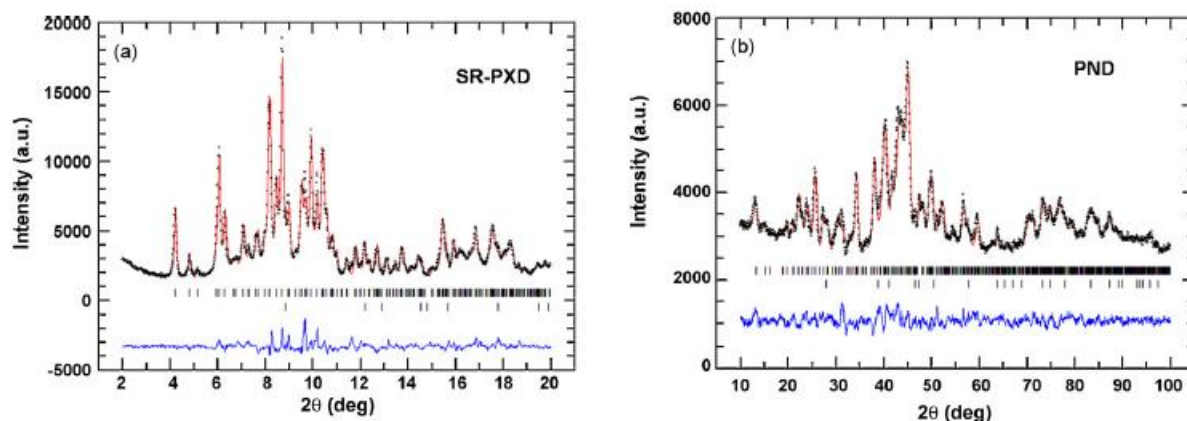


Figure 16: Rietveld refinement fits of $\text{Ca}(\text{BD}_4)_2$. Upper tick marks show Bragg peaks from $\text{Ca}(\text{BD}_4)_2$, the lower tick marks show Bragg peaks from AlD_3 .

The results have been published in Journal of Alloys and Compounds [5]

Hydride formation in Mg-based systems processed by reactive milling

The possibilities to produce quaternary Mg-based transition-metal complex hydrides have been explored. $\text{Mg}_2\text{Mn}_{1-x}\text{Fe}_x$ ($x = 0.5, 0$) elemental powder mixtures were ball milled in a reactive D_2 atmosphere (about 5 MPa). The results were compared with the formation of $\text{Mg}_2(\text{FeD}_6)_{0.5}(\text{CoD}_5)_{0.5}$ from Mg-Fe-Co powders.

High resolution SR-PXD performed at BM01B was used in conjunction with neutron diffraction for the structural characterization of the as-milled powders.

$\text{Mg}_2\text{Mn}_{0.5}\text{Fe}_{0.5}$ powder (Figure 17) showed a large fraction of unreacted elemental Mn, as well as the formation of a cubic K_2PtCl_6 -type phase ($a = 6.452 \text{ \AA}$). The latter could be identified as Mg_2FeD_6 . Infrared spectroscopy confirmed the presence of $[\text{FeD}_6]^{4-}$ anions (stretching band at 1261 cm^{-1}) and ruled out the formation of $[\text{MnH}_6]^{5-}$ complexes.

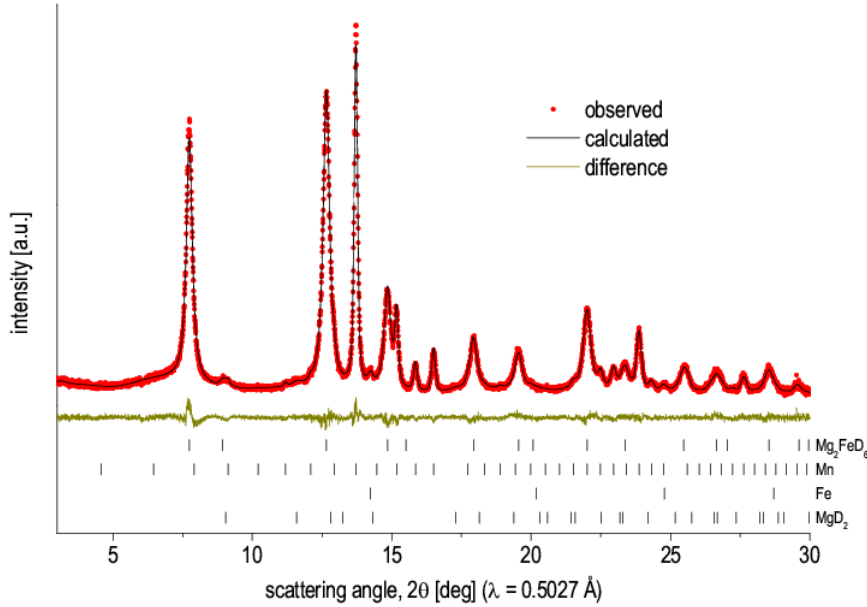


Figure 17: High-Resolution SR-PXD for $\text{Mg}_2\text{Mn}_{0.5}\text{Fe}_{0.5}$ ball milled in D_2 . The position of Bragg reflections for Mg_2FeD_6 , Mn, Fe, and MgD_2 are shown (bars) together with the observed pattern (solid circles) and the profile calculated by Rietveld refinement (solid lines).

High-resolution SR-PXD for as-milled Mg_2Mn (Figure 18) showed the formation of MgD_2 as the main reaction product. A small fraction of a cubic K_2PtCl_6 -type phase ($a = 6.526 \text{ \AA}$) was also observed. This was identified as an Mg_2FeD_6 -type compound. It was likely formed as a result of Fe impurities originating from the milling media. The large cell parameter suggests partial dissolution on Mn in the Mg_2FeD_6 -type phase. This is supported by the presence of an additional band at 1313 cm^{-1} in the IR spectrum.

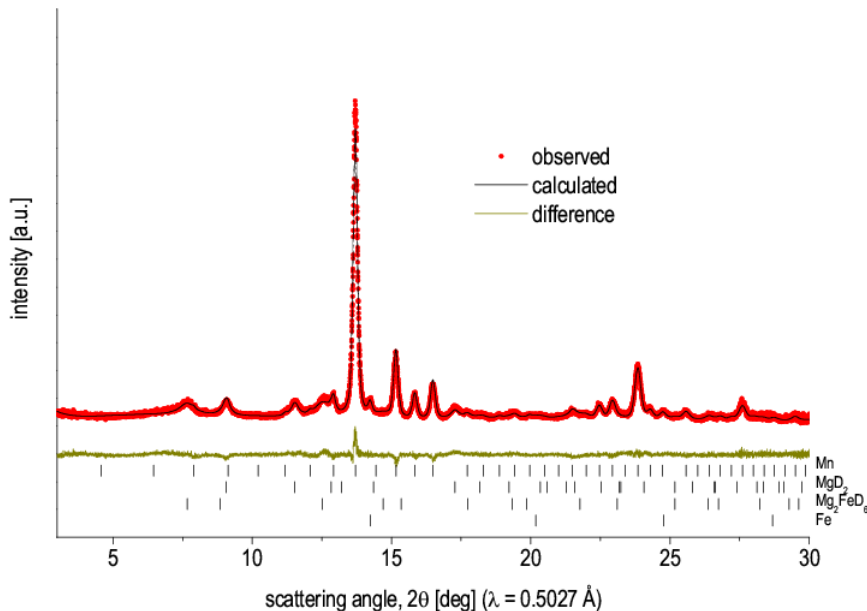


Figure 18: High-Resolution SR-PXD for $\text{Mg}_2\text{Mn}(\text{Fe})$ ball milled in D_2 . The position of Bragg reflections for Mg_2FeD_6 , Mn, Fe, and MgD_2 are shown (bars) together with the observed pattern (solid circles) and the profile calculated by Rietveld refinement (solid lines).

The results have been published in Faraday Discussion [6]

Structure determination of ϵ -Mg(BH₄)₂

Mg(BH₄)₂ has α - and β - polymorphs and the structures of these polymorphs have been reported. Recently, commercial Mg(BH₄)₂ has become available from Sigma-Aldrich, and the product is yet another polymorph, the so-called γ -phase. It was found that the γ -phase transforms to an intermediate phase (tentatively named ϵ -Mg(BH₄)₂) after heating to 170 °C. ϵ -Mg(BH₄)₂ then transforms to the β phase after heating up to 210 °C. To determine structure of ϵ -Mg(BH₄)₂, high resolution SR-PXD data of ϵ -Mg(BH₄)₂ was collected at BM01B at room temperature. Figure 19(a) shows HR-SR-PXD data of the sample after annealing of γ -Mg(BH₄)₂ at 160 °C under 1 MPa H₂ atmosphere. Since no diffraction peaks from γ -Mg(BH₄)₂ were observed, the profile is expected to be originated from ϵ -Mg(BH₄)₂, however, it may contain small amount of β -Mg(BH₄)₂. HR-SR-PXD data of γ -Mg(BH₄)₂ annealed at 210 °C under 1 MPa H₂ atmosphere (Figure 19(b)) shows the presence of β -phase without the odd-order reflections which would be observed as significantly weak and broad peak due to antisite disorder. Structure solution of ϵ -Mg(BH₄)₂ is currently in progress.

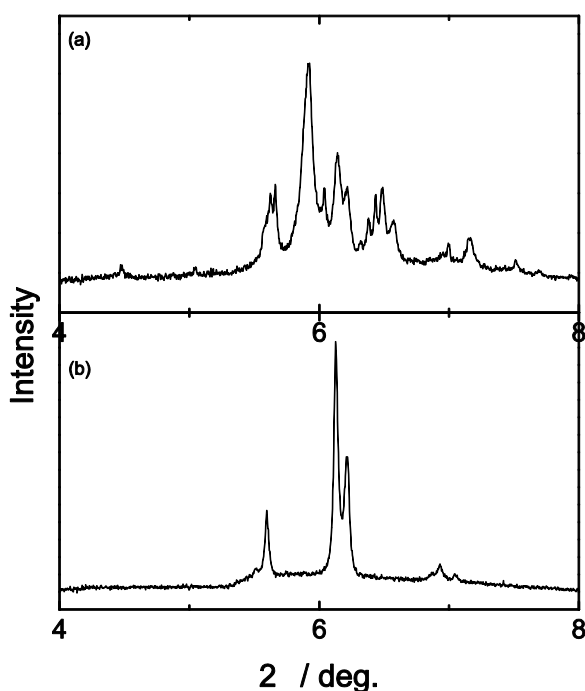


Figure 19: SR-PXD data ($\lambda = 0.502068 \text{ \AA}$) for (a) commercial Mg(BH₄)₂ annealed at 160 °C and (b) at 210 °C for 10 h under 1 MPa H₂ atmosphere.

Structure determination of ${}^7\text{Li}{}^{11}\text{BD}_4$

Powder neutron diffraction data (unpublished) recorded at the PUS instrument at the JEEP II reactor (Kjeller, Norway) suggest that the high-temperature polymorph of LiBH_4 might be more disordered than the structure model reported by Soulié et al (Soulié, J. P.; Renaudin, G.; Cerný, R.; Yvon, K. *J. Alloys Comp.* **2002**, 346, 200).

To determine the structure precisely, a triple-isotope substituted material, ${}^7\text{Li}{}^{11}\text{BD}_4$, was purchased due to the neutron absorption of natural boron and lithium and the high incoherent scattering of natural hydrogen.

High-resolution SR-PXD data were recorded for the low-temperature phase (ambient temperature) and the high-temperature phase (130 °C) for simultaneous structure refinement with PND data (Figure 20).

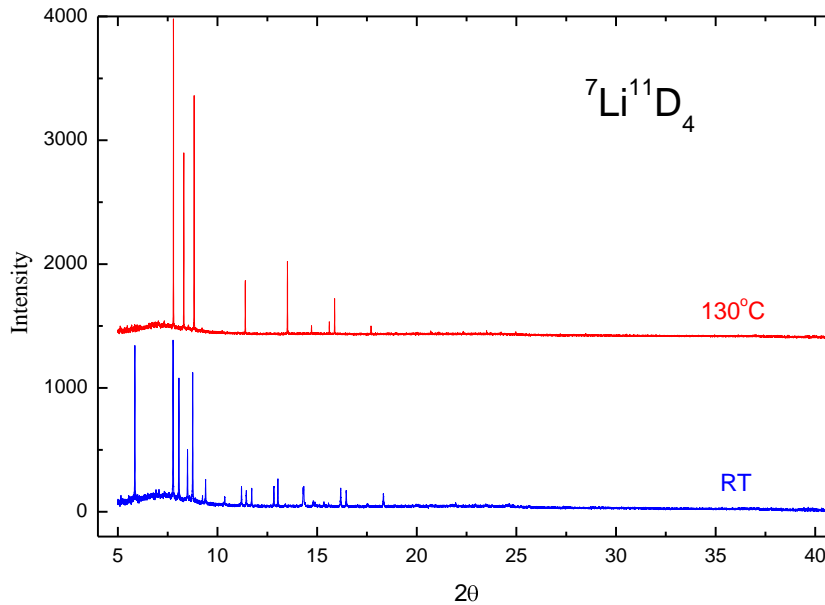


Figure 20: SR-PXD data for HT- (top) and RT-modification (bottom) of triple-isotope substituted LiBH_4 .

The analysis is currently still in progress.

Concluding remarks

The long-term project 01-01-805 has resulted in a total number of 6 publications and one submitted paper. The already collected data are expected to result in another 2 manuscripts in 2012.

Published papers with results from the long-term project

1. Riktor, M.D., et al., *The crystal structure of the first borohydride borate, Ca(3)(BD(4))(3)(BO(3))*. Journal of Materials Chemistry, 2011. **21**(20): p. 7188-7193.
2. Frommen, C., et al., *Crystal structure, polymorphism, and thermal properties of yttrium borohydride Y(BH₄)₃*. Journal of Alloys and Compounds, 2010. **496**(1-2): p. 710-716.
3. Frommen, C., et al., *Synthesis, Crystal Structure, and Thermal Properties of the First Mixed-Metal and Anion-Substituted Rare Earth Borohydride LiCe(BH(4))(3)Cl*. Journal of Physical Chemistry C, 2011. **115**(47): p. 23591-23602.
4. Fonnelløp, J.E., et al., *Experimental and computational investigations on the AlH₃/AlF₃ system*. Journal of Alloys and Compounds, 2011. **509**(1): p. 10-14.
5. Sato, T., et al., *Syntheses, crystal structures, and thermal analyses of solvent-free Ca(AlD₄)(₂) and CaAlD₅*. Journal of Alloys and Compounds, 2009. **487**(1-2): p. 472-478.
6. Deledda, S. and B.C. Hauback *Hydride formation in Mg-based systems processed by reactive milling*. Faraday Discussion, 2011. **DOI:10.1039/C1FD00023C**.